This article was downloaded by:
On: *14 January 2011*
Access details: *Access Details: Free Access*
Publisher *Taylor & Francis*
Informa Ltd Registered in England and Wales Registered Number: 1072954 Registered office: Mortimer House, 37-41 Mortimer Street, London W1T 3JH, UK

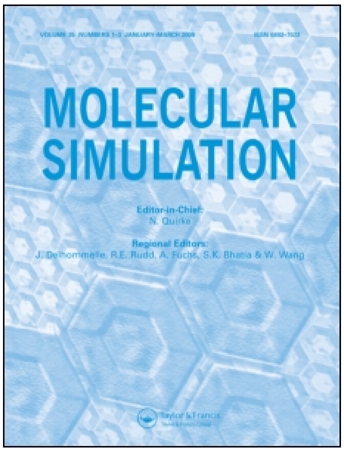

Molecular Simulation

Publication details, including instructions for authors and subscription information:
http://www.informaworld.com/smpp/title~content=t713644482

Inhibition of Ice Nucleus Growth in Water by Alanine Dipeptide

K. Iwasaki[a]; Y. Hagiwara[a]
[a] Department of Mechanical and System Engineering, Kyoto Institute of Technology, Kyoto, Japan

To cite this Article Iwasaki, K. and Hagiwara, Y.(2004) 'Inhibition of Ice Nucleus Growth in Water by Alanine Dipeptide', Molecular Simulation, 30: 8, 487 — 500

To link to this Article: DOI: 10.1080/08927020410001713951

URL: http://dx.doi.org/10.1080/08927020410001713951

PLEASE SCROLL DOWN FOR ARTICLE

Full terms and conditions of use: http://www.informaworld.com/terms-and-conditions-of-access.pdf

This article may be used for research, teaching and private study purposes. Any substantial or systematic reproduction, re-distribution, re-selling, loan or sub-licensing, systematic supply or distribution in any form to anyone is expressly forbidden.

The publisher does not give any warranty express or implied or make any representation that the contents will be complete or accurate or up to date. The accuracy of any instructions, formulae and drug doses should be independently verified with primary sources. The publisher shall not be liable for any loss, actions, claims, proceedings, demand or costs or damages whatsoever or howsoever caused arising directly or indirectly in connection with or arising out of the use of this material.

Molecular Simulation, Vol. 30 (8), 15 July 2004, pp. 487–500

Taylor & Francis
Taylor & Francis Group

Inhibition of Ice Nucleus Growth in Water by Alanine Dipeptide

K. IWASAKI and Y. HAGIWARA*

Department of Mechanical and System Engineering, Kyoto Institute of Technology, Goshokaido-cho, Matsugasaki, Kyoto 606-8585, Japan

(Received October 2003; In final form April 2004)

A molecular dynamics simulation has been carried out for the mixture of an ice nucleus, supercooled water and a molecule of alanine dipeptide (AD). The dipeptide molecule has been allocated near the nucleus surface which corresponds to the prism plane of ice crystal. The molecule is found to approach the ice surface so that the two hydrophilic sites on one side of the molecule (Oc2 and Hn1) are closest to the surface. The hydrogen bond between Hn1 site and the oxygen atom on the prism plane of the ice nucleus is expected. The perturbations of two hydrophilic sites (Oc1 and Hn2), which are surrounded by hydrophobic sites and are pointing away from the surface, attenuate the approach of water molecules to these sites. Thus, these water molecules diffuse. The hydrogen bond between the oxygen atoms on the prism plane and the hydrogen atoms of water molecules is attenuated by the diffusion.

Keywords: Ice Ih structure; Alanine dipeptide molecule; Hydrogen bond; Water-molecule clustering

INTRODUCTION

Utilizing antifreeze protein (AFP) or antifreeze glycoprotein for cooling and freezing processes has been the focus of recent research. This is because these proteins are effective for lowering the freezing temperature and attenuating the growth of ice crystals. Also, they are obtained from certain kinds of fish and are non-toxic. To reduce the ice crystal growth is the key for the improvement in taste of dairy products and frozen meat [1]. The inhibition of ice crystal growth is crucial for the storage of internal organs for surgery in hospitals. Also, the control of ice growth is directly applicable for producing microparticle ice slurry, which is effective for heart and brain cooling during cardiac arrest.

Among the proteins, the AFP type I has been investigated widely because this AFP has a lower molecular mass (3300–4500 Daltons) compared with the other proteins. The structure of the AFP has been clarified with X-ray microscope [2]. The AFP type I from winter flounder (HPLC6) forms α-helix and has 37 residues. The alanine residue constitutes the largest amount of these residues. It was also found that the ice crystals grew in the specific direction in the AFP solution. A hypothesis for HPLC6 has been developed and (until recently) accepted based on observations and computational studies on protein–ice interactions *in vacuo*. The polar (hydrophilic) residues, threonine (Thr2, Thr13, Thr24, Thr35), asparagines (Asn16, Asn27) and aspartate (Asp5), adsorbed preferentially on the prism surface of the ice crystal by hydrogen bond, and thus, many residues of alanines (the hydrophobic residues), which oriented away from the ice surface, interfered with the approach of water molecule in the liquid phase to the surface [3].

New experimental or computational results disproving the hypothesis have been obtained over the past seven years. Chao *et al.* [4] and Haymet *et al.* [5] discovered that the synthetic AFP type I analog, in which the threonine residues were replaced with the hydrophobic valine residues, showed similar activity of lowering the freezing temperature. Dalal *et al.* [6] investigated the effect of the HPLC6 molecule on the water molecules in the liquid phase near the pyramidal plane of the ice crystal with a molecular dynamics simulation. They concluded that there was no gain of hydrogen bonds when the protein interacted with the ice–water interfacial region. They also showed that the vacuum is a very poor

---

*Corresponding author. E-mail: yoshi@kit.ac.jp

ISSN 0892-7022 print/ISSN 1029-0435 online © 2004 Taylor & Francis Ltd
DOI: 10.1080/08927020410001713951

approximation for the properties of water. Furthermore, DeLuca *et al.* [7] put forward a new hypothesis in which many hydrophobic residues of AFP type III adsorbed on the interface.

As far as the present authors know, the effect upon the ice crystal of three alanine residues in HPLC6 (Ala9, Ala20, Ala31), which are nearly aligned with the seven hydrophilic residues mentioned above in the linear helical structure of the HPLC6, has not yet been discussed in detail. Ala9 has the peptide bond on both sides with Ala8 and Ala10, and Ala31 also has the peptide bond on both sides with Ala30 and Ala32. In these alanine polypeptides, the hydrogen site and the oxygen site can be positioned close to the ice lattice. This combination of hydrophilic sites has a potential for bonding with the ice lattice. To examine the behaviors of Ala9, Ala20 and Ala31 is not enough for elucidating the interaction between these hydrophilic sites and the ice lattice because these residues are affected by the other hydrophilic residues aligned. It is valid to examine the behavior of a sole alanine polypeptide model near the ice lattice.

This study aims at elucidating the interaction among a cubic nucleus of ice Ih crystal, a molecule of alanine dipeptide (AD) and surrounding water with a molecular dynamics simulation. This ice nucleus, which is the same as that formed in our previous study [8], has specific prism planes of crystal associated with ice growth. Also, the nucleus has an advantage in that it reduces the effect of the boundary of computational domain on the motion of molecules near the ice–water interface. In addition, the ice nucleus can be considered as a nucleus just formed around a particle, which is the seed of the phase change, though we do not include any particle inside the nucleus. The AD molecule is a well-defined, small polypeptide. Inconsistency due to the introduction of polypeptide into the computational domain can be reduced by using this small AD molecule. The effects of hydrophilic or hydrophobic sites of the AD molecule on the water molecules near the ice lattice on the specific prism plane are discussed.

SIMULATION METHOD

We used the computer program developed in our previous study [8].

Assumptions

The classical molecular dynamics simulation was applied. It was assumed that the number of molecules, the volume of computational domain and the total energy were kept constant (hereafter called the *NVE* ensemble) except for heating or energy removal procedures mentioned below. All the molecules were assumed as rigid bodies. The net dipole moment, which was discussed by Hayward and Reimers [9], was not evaluated. The periodic boundary condition was imposed on the computational domain.

Potential Functions of Water Molecules

The TIP4P potential [10] was adopted for the potential function for the interaction between two water molecules. The potential function consists of the Coulomb potential and the Lennard–Jones potential.

The cutoff of the force acting on two distant molecules was carried out with the following methods: the cutoff radius for the Lennard–Jones potential and the Ewald method [11] for the Coulomb potential. The cutoff radius was set at 2.245 nm, which was equal to a dimension of the ice nucleus. The parameters for the Ewald summation were $\alpha = 5.6$, $|\mathbf{u}_y|_{\max} = 1$, $|\mathbf{h}_y|_{\max} = 5$ where α is the width of the Gaussian distribution, $\mathbf{u}_y$ is the vector for the location of image cell in the y-direction in the physical space, and $\mathbf{h}_y$ is the vector for the location of image cell in the Fourier space.

Time Integral

The Newton–Euler equations for the translational and rotational motions were solved at each time step, and were integrated with the Gear algorism [12], a one-step predictor–corrector method. We adopted 5-value Gear algorism in which the time derivatives up to the fifth order are considered for the second-order differential Newton–Euler equation for the translational motion. We also used 4-value Gear algorism for the second-order differential equation for the rotation. All the computations were carried out with the time step of 0.5 fs.

Estimation and Adjustment of Temperature

The statistical temperature T, was given with the law of equi-partition of energy by the total energy of the translational motion for all the molecules K_T, and that of the rotational motion for the molecules K_R. The temperature is written as follows:

$$\begin{aligned} T &= \frac{1}{2}\left(\frac{2}{3k_BN}K_T + \frac{2}{3k_BN}K_R\right) \\ &= \frac{1}{3k_BN}\left(\frac{1}{2}\sum_{i=1}^{N} m\mathbf{v}_i^2 + \frac{1}{2}\sum_{i=1}^{N}\left(I_{px_i}\omega_{px_i}^2 + I_{py_i}\omega_{py_i}^2 \right.\right. \\ &\qquad \left.\left. + I_{pz_i}\omega_{pz_i}^2\right)\right), \end{aligned} \tag{1}$$

where k_B is the Boltzmann constant, N is the total number of molecules, m is the mass of molecules, and I_p is the inertia based on its principal axis. The temperature scaling was done by changing the translational velocity **v**, and the angular velocity ω, of each molecule with the following equation:

$$\mathbf{v}_i^{(\text{new})} = \mathbf{v}_i^{(\text{old})}\sqrt{\frac{T_{pd}}{T_0}},\ \boldsymbol{\omega}_i^{(\text{new})} = \boldsymbol{\omega}_i^{(\text{old})}\sqrt{\frac{T_{pd}}{T_0}}, \qquad (2)$$

where T_0 is the present temperature and T_{pd} is the predetermined temperature.

MIXTURE OF ICE AND WATER

The result obtained in our previous study [8] for the mixture of supercooled water with a cubic ice nucleus was used as the initial condition for the preliminary computation of the present study. Two prism planes of ice crystal are realized by the cubic ice nucleus, though a pyramidal plane for the crystal cannot be realized. Furthermore, the nucleus has an advantage in that the motion of molecules is not affected noticeably by the mirror images due to the periodical boundary condition. The outline of the procedure to obtain the mixture is described below.

Formation of Ice

Three-hundred and sixty water molecules were arranged in a cubic domain based on the ice Ih structure. Six horizontal planes were considered in the domain. Sixty molecules were positioned so that the hexagonal structure was formed on each plane. The z-axis of the Cartesian coordinate was allocated in the upward direction and normal to the planes. This axis and the top plane corresponded to the c-axis and the $\{0001\}$ basal plane of the hexagonal crystal of ice Ih structure, respectively. The y-axis was allocated in parallel with the a_2-axis. Then, the two boundaries normal to the x-axis were considered as the $\{10\bar{1}0\}$ and $\{\bar{1}010\}$ prism planes. Water molecules are adsorbed by these planes during the freezing process.

The rotational angle for each molecule at the initial state was given randomly. The Newton–Euler equations were solved with the proper constraint condition for the molecular displacement and the temperature scaling. It was confirmed from the self-diffusion function, the radial distribution function and snapshots that the ice Ih crystal state was sustained in the cases of temperatures lower than 265 K.

Production of Ice–water Mixture

The new computational domain whose dimension was twice as large as that used above in the three directions was filled with eight identical ice crystals. The origin of the coordinate was shifted at the center of this large computational domain. Only one of the crystals located near a lower corner of the domain ($-2.245 \le x \le 0$, $-2.333 \le y \le 0$, $-2.200 \le z \le 0$ nm) was used as the ice nucleus, and the rest was melted by gradual heating and used for the liquid region. Through the heating, the temperature scaling was applied intermittently for the translational velocity of each molecule in the liquid region so that the water temperature reached a predetermined temperature. The heating continued until the predetermined temperature was equal to a target temperature. The total energy input was approximately 90% of the latent heat.

Mixture of Ice and Supercooled Water

We removed the energy from the liquid region gradually in order to obtain the supercooled water. A similar procedure to that used for the melting of ice mentioned above was applied for the energy removal procedure: Through the cooling process, the temperature scaling was applied intermittently for the translational velocity of each molecule in the liquid region so that the water temperature reached a predetermined temperature. The removal of energy continued until the predetermined temperature was equal to the target temperature of 240 K. The total energy removed was approximately 50% of the latent heat.

After the energy removal procedure, the interaction between the ice nucleus and the supercooled water was started. The initial state for the present simulation was the result at 100 ps after the initiation of the interaction between ice nucleus and the supercooled water. The average energies and the average temperature for 5 ps just before the initial state are shown in Table I.

The computation without the AD molecule was also carried out in order to obtain reference data for the discussion of the effects of the AD molecule on water molecules.

Near-ice Region

The liquid phase was divided into two regions: the near-ice region and the far-ice region. The near-ice region covered the whole surface of the ice nucleus. The thickness of the region was 0.75 nm.

TABLE I Mean values of potential energy, translational temperature and rotational temperature for ice and water

	Ice nucleus	*Liquid region*
Potential energy (kJ/mol)	−48.2	−45.1
Translational kinetic energy (kJ/mol)	3.02	3.01
Translational temperature (K)	242.3	241.5
Rotational kinetic energy (kJ/mol)	3.11	3.00
Rotational temperature (K)	249.2	240.4

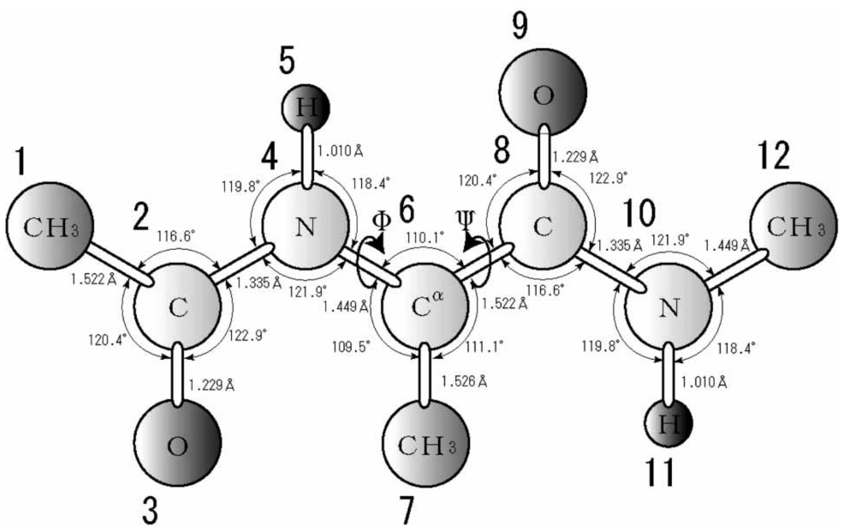

FIGURE 1 AD molecule.

AD MOLECULE

Assumptions

The AD molecule was assumed to be rigid and thus its configuration was unchanged through the computation for simplicity. Therefore, no natural frequency exists for the AD molecule.

Conformation Parameters

Figure 1 shows the AD molecule. The OPLS parameters obtained by Jorgensen and Tirado-Rives [13] were adopted to the potential parameters for each site of the AD molecule. The parameters are summarized in Table II. The center of mass of the molecule was close to the α-Carbon, C^{α} (site #; 6, type; CH). The electric charge and potentials for one of the CH_3 site (site #; 12, type; JW) were different from those of the other hydrophobic sites of C31 and C32 in order to reduce the end effect of the AD molecule. Note that the hydrophilic sites of Oc1 and Oc2 do not appear in alanine but in the AD molecule.

The dihedral angle around the C^{α}—N bond φ, and that around the C^{α}—C bond ψ, were determined so that the AD molecule took the α-helix conformation. According to the Ramanchandran plots and the result obtained by Gould *et al.* [14], we set $\varphi = -60.7$ degrees and $\psi = -40.7$ degrees. These values were approximately equal to the average values of 20 alanine residues in HPLC6.

Introduction of AD Molecule into Water

A number of water molecules were removed from a spherical domain in the near-ice region. The domain was adjacent to one of the surfaces, which corresponded to the $\{10\bar{1}0\}$ prism plane. The AD molecule was introduced into the vacancy. The radius of domain was set equal to the length of the longer axis of the AD molecule. The total number of water molecules removed was 21. The computational condition is summarized in Table III. The translational and rotational velocities of the AD molecule were set equal to zero at the initial state.

We selected two different initial orientations for AD molecule in order to examine the effect of the initial condition of orientation on the results. The basic difference between the two cases was that the two hydrophilic sites of Oc2 and Hn1 were oriented away from the ice surface (Case 1) or to the ice surface (Case 2). The initial coordinates of the four sites (Oc1, Oc2, Hn1 and Hn2) are

TABLE II Parameters for AD molecule

	Site #	*Site type*	*q*	*a(nm)*	*ε (kJ/mol)*
Hydrophobic sites	1, 7	C31, C32	0.0	0.391	0.670
	12	JW	0.2	0.38	0.712
Hydrophilic sites	2, 8	C1, C2	0.5	0.375	0.440
	3, 9	Oc1, Oc2	−0.5	0.296	0.879
	4, 10	N1, N2	−0.57	0.325	0.712
	5, 11	Hn1, Hn2	0.37	0	0
	6	CH	0.2	0.38	0.335

TABLE III Computational condition

Domain (nm^3)	4.491 × 4.667 × 4.400
Time step (fs)	0.5
Number of molecules in ice nucleus	360
Number of molecules in liquid region	2499
Number of AD molecule	1
Initial temperature of ice nucleus (K)	245.1
Initial temperature of liquid region (K)	239.3
Predetermined temperature of ice nucleus (K)	245.8
Predetermined temperature of liquid region and AD (K)	241.0

shown in Table IV. The distance between any site and water molecules in the ice nucleus is longer than the length for hydrogen bond. Figure 2 shows the initial location of the AD molecule for the Case 1.

The temperature scaling was carried out after the AD molecule was introduced in order to attenuate an unrealistic rapid increase in the energy due to the inconsistency of the potentials of the molecules. The scaling procedure was summarized in Table V. For the first 5 ps, the molecules in ice were fixed and the displacement of the AD molecule was reduced to 0.1% of its predicted value. The temperature scaling was carried out at each time step. For the next 5 ps (5–10 ps), the displacements of the molecules in ice and the AD molecule were reduced to 0.1% of their predicted value. The scaling was carried out at each time step. For the third 5 ps (10–15 ps), only the scaling was carried out at each time step. The temperature scaling was terminated at the end of this step.

The near-ice region defined in the above was divided into two sub-regions: the near-AD region and the far-AD region. The former is the near-ice region facing to the ice surface corresponding to the $\{10\bar{1}0\}$ prism plane, in which the AD molecule was allocated. The latter is that facing to the ice surface corresponding to the $\{\bar{1}010\}$ prism plane.

TABLE IV Initial coordinates of Oc and Hn sites

	Site type	(x, y, z) (nm)
Case 1	Oc1	(0.242, − 1.255, − 0.842)
	Oc2	(0.499, − 1.272, − 1.212)
	Hn1	(0.491, − 1.053, − 1.016)
	Hn2	(0.302, − 1.087, − 1.359)
Case 2	Oc1	(0.314, − 1.439, − 0.981)
	Oc2	(0.523, − 1.046, − 1.050)
	Hn1	(0.234, − 1.084, − 1.017)
	Hn2	(0.443, − 1.054, − 1.348)

SELF-DIFFUSION FUNCTION

In order to judge whether the system is in a liquid state or an ice state, we used the self-diffusion function defined by the following equation:

$$D(t) = \frac{1}{N}\sum_{i=1}^{N} (\mathbf{r}_i(t) - \mathbf{r}_i(0))^2, \qquad (3)$$

where $\mathbf{r}_i(t)$ is the coordinate of a molecule i at time t. If the function increases with time, the system is in a liquid state. If the function increases gradually with time, the motion of molecules is restricted by the adsorption of molecules to solid surface due to the solidification. If the function keeps nearly equal to zero, the system is in a solid state.

RESULTS AND DISCUSSION

Total Energy of System

It was confirmed that the total potential energy and the total kinetic energy were kept constant throughout the computation. Thus, the present computation based on the micro-canonical (*NVE*) ensemble was validated. Furthermore, the system was confirmed to be stable.

Interaction between Ice Nucleus and AD Molecule

Motion of AD Molecule

Figure 3 shows the time changes in the x-coordinates of seven sites and the x, y and z coordinates of the center of mass for the AD molecule in Case 1. The x-coordinates of the C31, Hn1 and Oc1 sites decreased noticeably for the period of 22–40 ps. On the other hand, the x-coordinates of Hn2 and JW sites fluctuated around their mean values for this period. This shows that the left side of the AD molecule shown in Fig. 1 approached the ice surface, while the right side of the molecule stayed around the same location. For the period of 40–85 ps, the x-coordinates of the Hn1 and C31 sites increased gradually and the other sites stayed around the same location. The C31, Oc2 and Hn1 sites were closer to the ice surface than the other sites for this period, which shows that the upper side of the AD molecule in Fig. 1 was close to the surface. The mean value in the x-coordinate of the Oc2 site for this period was approximately 0.2 nm, and that of the Hn1 site was approximately 0.3 nm.

For the period of 85–125 ps, the x-coordinates of the JW, Oc2 and Hn2 sites increased more than before, while those of the other sites increased less than before. This indicates that only the right side of the AD molecule in Fig. 1 moved gradually away from the surface. The time change in the x, y

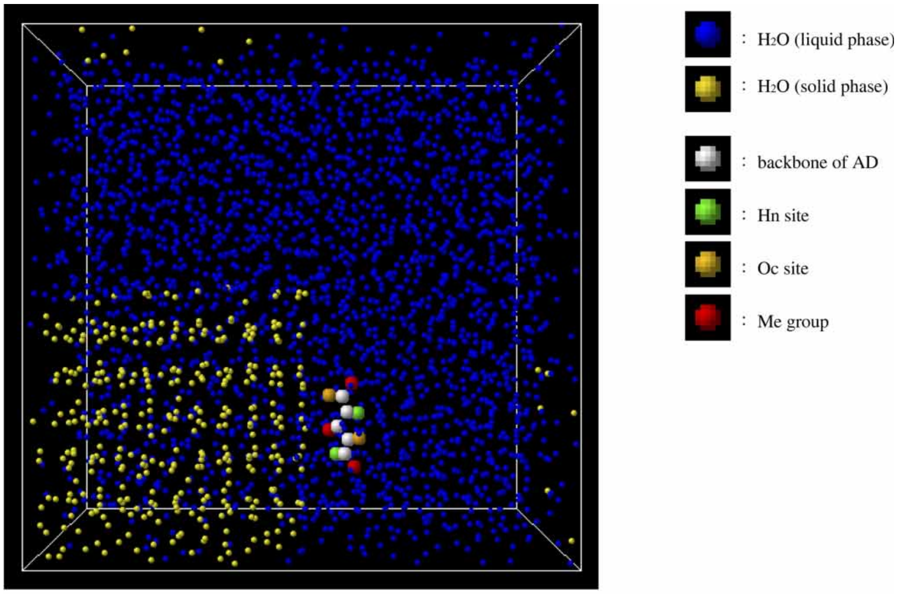

(a) view from y-axis

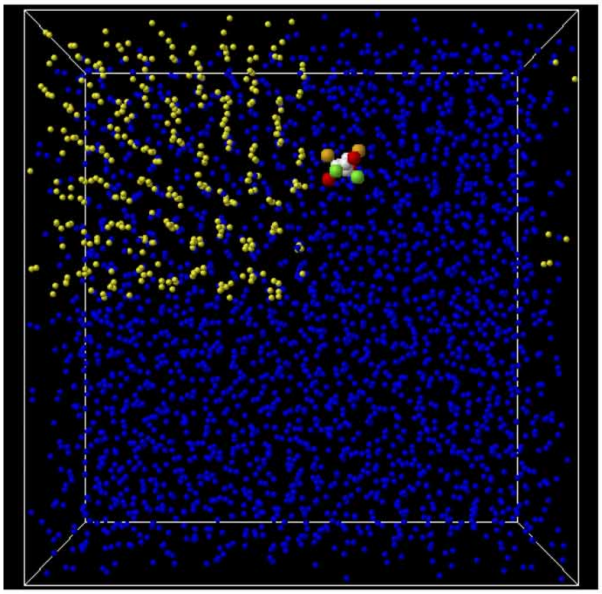

(b)view from z-axis

FIGURE 2 Snapshot for the initial condition in Case 1. (Colour version available online.)

and z coordinates for the center of mass was not noticeable in this period. The mean value in the x-coordinate of the Oc2 site for this period was approximately 0.25 nm, and that of the Hn1 site was approximately 0.35 nm. After 125 ps, the C31 and Hn1 sites moved away from the surface, while the other site moved towards the surface. Thus, the three-dimensional perturbation of the position of the AD molecule was observed through the periods.

TABLE V Scaling procedure

Period	*Liquid region*	*Ice nucleus*	*AD molecule*	*Scaling interval*
0–5 (ps)	Free	Fix	0.1%	0.5 (fs)
5–10 (ps)	Free	0.1%	0.1%	0.5 (fs)
10–15 (ps)	Free	Free	Free	0.5 (fs)
15–95 (ps)	Free	Free	Free	–

Figure 4 indicates the time changes in the x-coordinates of seven sites and the x, y and z coordinates of the center of mass for the AD molecule in Case 2. The x-coordinates of the JW, Oc2 and Hn2 sites decreased noticeably for the period of 25–80 ps. On the other hand, the x-coordinates of Oc1 and C31 sites decreased gradually for this period. This shows

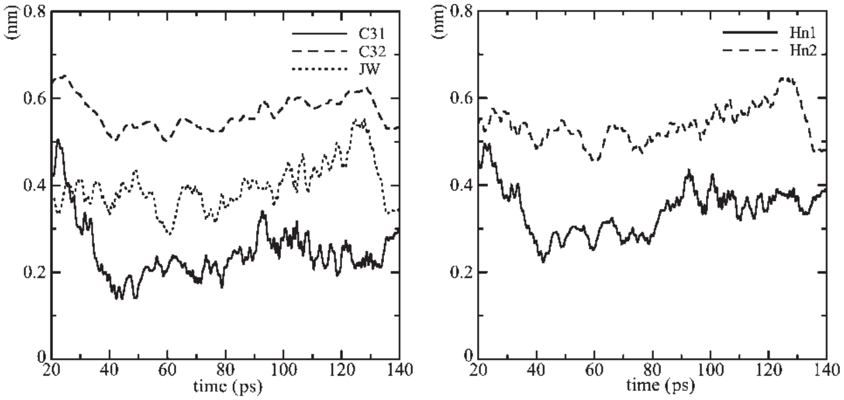

(a) Me group

(b) Hn site

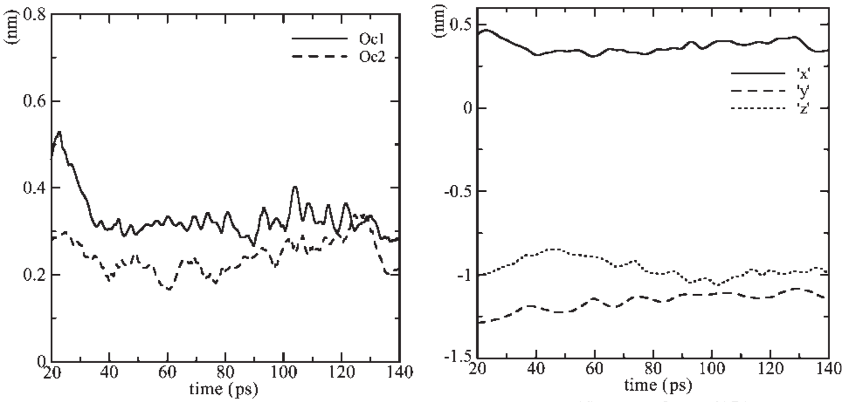

(c) Oc site

(d) center of mass (AD)

FIGURE 3 Time changes in the coordinates in Case 1.

that the right side of the AD molecule in Fig. 1 approached the ice surface, while the left side of the molecule remained in the same location for this period. Furthermore, the JW, Hn1 and Oc2 sites were closer to the ice surface than the other sites for the period of 40–80 ps. Hence, the Hn1 and Oc2 hydrophilic sites were closer to the ice surface for 40–80 ps irrespective of the initial allocation of the AD molecule. The mean value in the x-coordinate of the Oc2 site for this period was approximately 0.3 nm, and that of the Hn1 site was approximately 0.27 nm in this period. The interaction between the Hn1 site and the oxygen atom in the ice is stronger than that between the Oc2 site and the hydrogen atom in the ice.

For the period of 80–120 ps, the x, y and z coordinates for the center of mass fluctuated around their mean values, which are approximately equal to those in Case 1. In this period, the JW, Oc2 and Hn1 sites were still closer to the surface than the other sites, which is also similar to that in Case 1. The mean value in the x-coordinate of Oc2 site for the period was approximately 0.2 nm, and that of Hn1 was approximately 0.2 nm. These values were lowest in all the periods of Case 1 and Case 2. Therefore, the interaction between the ice and the Oc2 and Hn1 sites was the strongest for the period.

Mechanism of Ice–AD Interaction

We examined the distances between the atoms of water molecules and each site of AD molecule at every 10 ps in order to understand the ice–AD and water–AD interactions. Figure 5a,c and e depict the number of oxygen atoms inside the spherical regions for two Hn sites and the C32 site as a function of the radius r_s at 110 ps in Case 1. The snapshot at this moment is shown in Fig. 6. Figure 5b and d depict the number of hydrogen atoms inside the spherical regions for two Oc sites as a function of r_s at 110 ps in Case 1. The shaded bars show the number of atoms for water molecules in the solid phase, while the white bars show the number of atoms for water molecules in the liquid phase. It is found from Fig. 5a that one oxygen atom for a water molecule in the liquid phase was inside the spherical region of $r_s = 0.26$ nm for the Hn1 site, while no oxygen atom for a water molecule in the solid phase was inside the region. This radius is the radius for the first hydration shell for Hn sites obtained by Kalko *et al.* [15]. The average number of oxygen

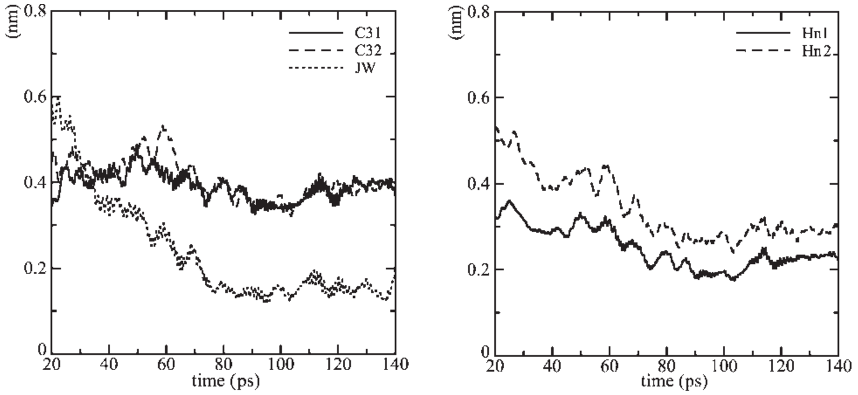

(a) Me group (b) Hn site

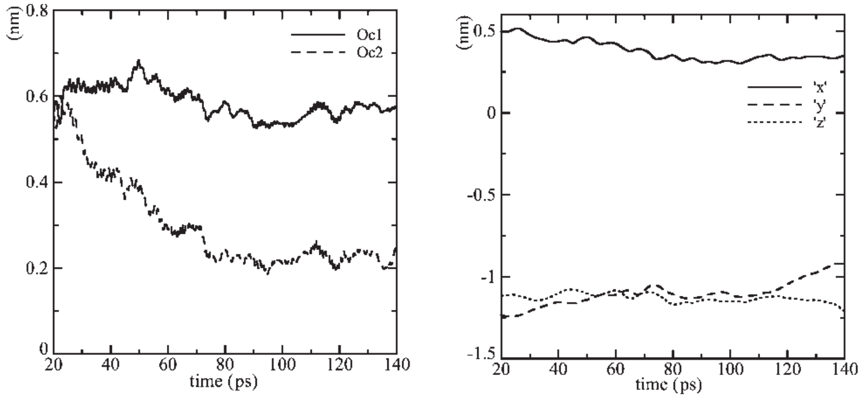

(c) Oc site (d) center of mass (AD)

FIGURE 4 Time changes in the coordinates in Case 2.

atoms inside the region was 0.8 for the period of 80–120 ps.

Two hydrogen atoms for a water molecule on the ice surface were found to be inside the spherical region for the Oc2 site ($r_s = 0.40\,\mathrm{nm}$; the radius for the first hydration shell for Oc sites) in Fig. 5b. The average number of hydrogen atoms in the ice nucleus inside the region was 1.8 for the period. The distance between the Oc2 site and the nearest hydrogen atom was 0.32 nm during the period of 60–120 ps. This distance is approximately equal to the *x*-coordinate of the Oc2 site mentioned above. Thus, the nearest hydrogen atom was located on the ice surface. The distance is longer than the hydrogen-bond length inside the ice, but shorter than the distance between the oxygen atom of a water molecule on the ice surface and the hydrogen atom of another water molecule on the ice (See Table VI). Furthermore, the angle for $(\mathrm{Ow{=}Hw})_{\mathrm{ice}}\cdots\mathrm{Oc2}$ is not 180 degrees, while the hydrogen bond of $(\mathrm{Ow{=}Hw}\cdots\mathrm{Ow})_{\mathrm{ice}}$ inside the ice takes 180 degrees. Therefore, the interaction between the Oc2 site and the hydrogen atom on the ice surface is weaker than the hydrogen bond between the ice and adsorbing water molecule.

Figure 7a,c and e indicate the number of oxygen atoms inside the spherical regions for two Hn sites and the C32 site as a function of the radius r_s at 90 ps in Case 2. Figure 7b and d indicate the number of hydrogen atoms inside the spherical regions for two Oc sites as a function of r_s at 90 ps in Case 2. There was one hydrogen atom for a water molecule in the liquid phase and one hydrogen atom for a water molecule on the ice surface was inside the spherical region of $r_s = 0.40\,\mathrm{nm}$ for the Oc2 site as shown in Fig. 7b. The average number of hydrogen atoms inside the region was 1.8 (0.8 in the solid phase and 1.0 in the liquid phase) for the period of 80–120 ps.

In contrast with Case 1, there was one oxygen atom for a water molecule in the ice nucleus inside the region of $r_s = 0.26\,\mathrm{nm}$ for the Hn1 site as shown in Fig. 7a. This oxygen atom stayed inside the region through the period of 80–120 ps. The distance between the Hn1 site and the nearest oxygen atom was approximately 0.21 nm during the period of 60–120 ps. This distance is approximately equal to the *x*-coordinate of the Hn1 site mentioned above. Thus, the nearest oxygen atom was located on the ice surface. The distance is approximately 24% longer than the length for the hydrogen bond inside the ice, and much shorter than the distance between the oxygen atom of a water molecule and the hydrogen

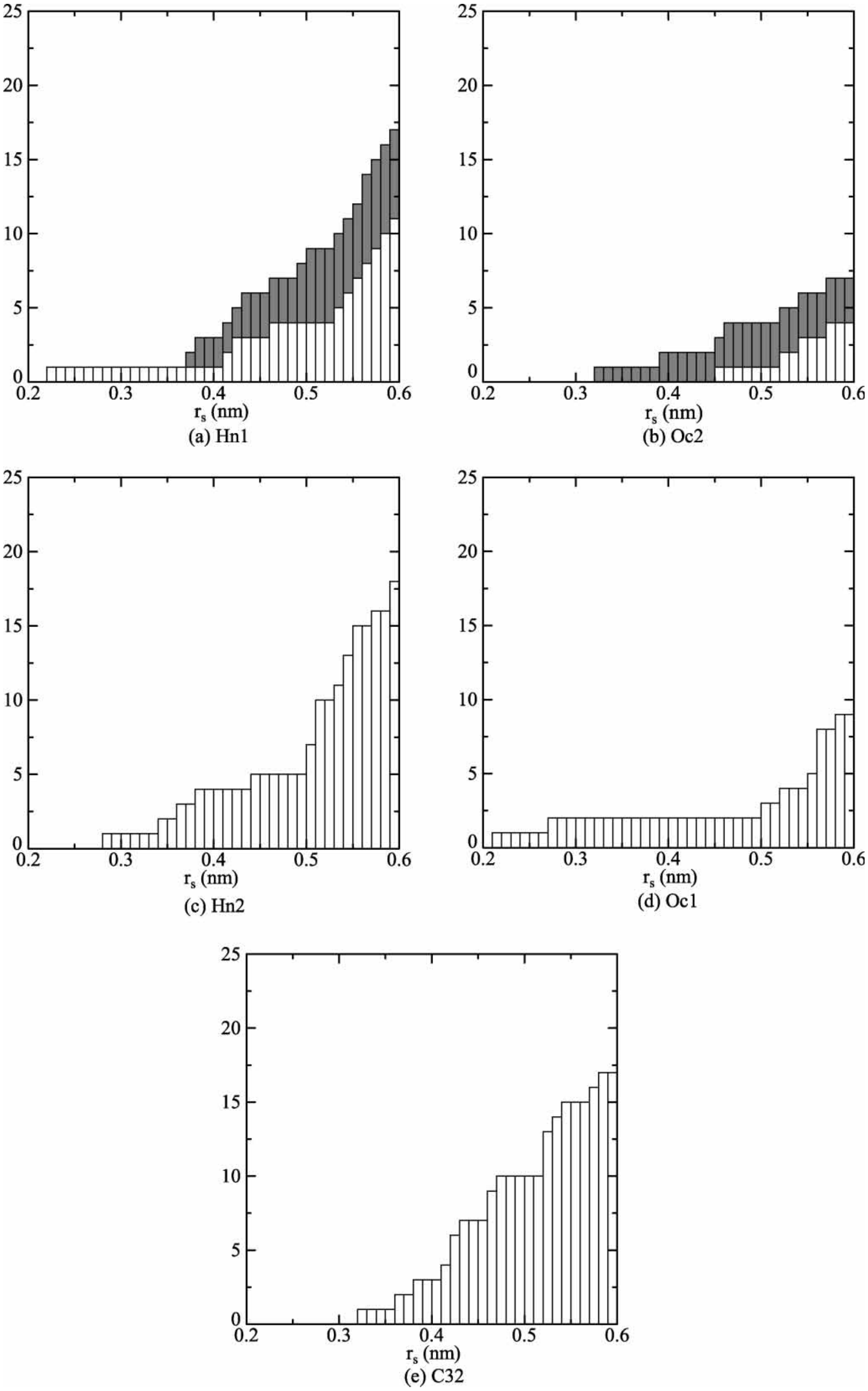

(a) Hn1

(b) Oc2

(c) Hn2

(d) Oc1

(e) C32

FIGURE 5 Number of atoms inside spherical shell in Case 1.

atom of another water molecule (See Table VI). The hydrogen bond of $(Hw{=}Ow)_{ice}\cdots Hn1$ takes approximately 120 degrees, which can be realized easily. Therefore, the Hn1 site can stay in its stable position very close to the ice surface in this type of hydrogen bond. This situation is drawn schematically in Fig. 8. The difference in the ice–AD interaction in Case 1 and that in Case 2 is related to the water–AD interaction mentioned above.

Interaction between AD Molecule and Water

Oc1 and Hn2 Sites

The Hn2, JW and C32 sites were farther from the ice nucleus than the other sites for the period of 30–120 ps in Case 1 as shown in Fig. 3. Thus, these sites were surrounded by water molecules in the liquid phase. Note that no oxygen atom was inside the spherical region of $r_s = 0.26\,\text{nm}$

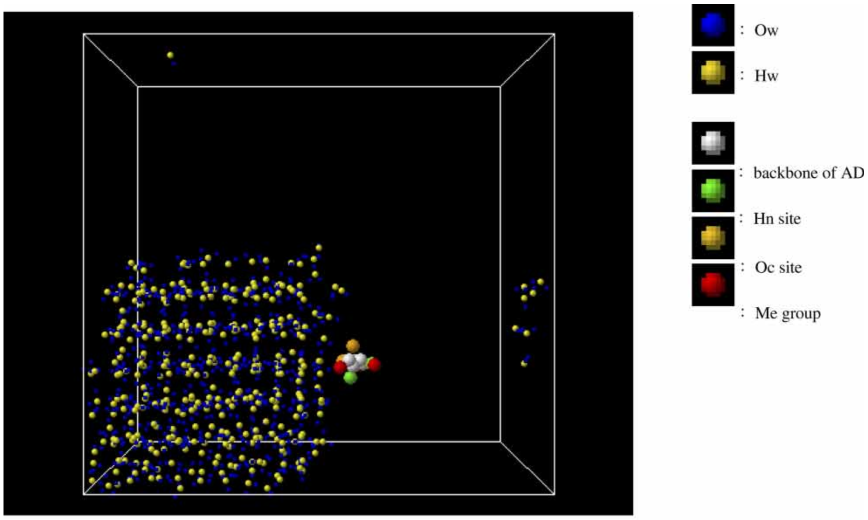

(a) view from y-axis

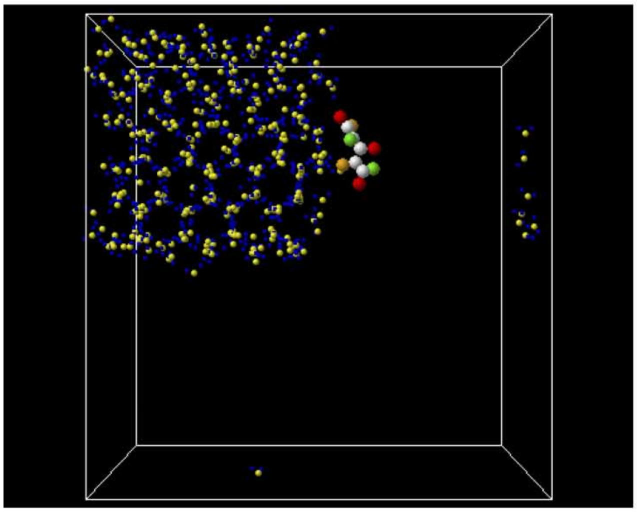

(b) view from z-axis

FIGURE 6 Snapshot at 110 ps in Case 1. (Colour version available online.)

TABLE VI Distances between oxygen atom and hydrogen atom

Inside ice crystal	
$(Ow{=}Hw)_{ice}$ (covalent bond; TIP4P)	0.096 nm
$(Ow\cdots Hw)_{ice}$ (hydrogen bond on the prism plane)	0.17 nm
$(Ow{-}Hw)_{ice}$ (between two water molecules on the prism plane)	0.34, 0.38,… nm
Sites of AD molecule	
Hn1—Oc2	0.30 nm
Oc1—Hn2	0.55 nm
Possible hydrogen bond between sites of AD molecule and ice crystal	
Case 1 (95–110 ps)	
$Oc2\cdots(Hw{=}Ow)_{ice}$	0.32 nm
$Hn1\cdots(Ow{=}Hw)_{ice}$	0.37 nm
Case 2 (95–110 ps)	
$Oc2\cdots(Hw{=}Ow)_{ice}$	0.35 nm
$Hn1\cdots(Ow{=}Hw)_{ice}$	0.21 nm

for the Hn2 site through this period except at 130 ps when one oxygen atom for a water molecule in the liquid phase was inside this region (figure omitted). This shows the difficulties in the hydrogen bond between the Hn2 site and the oxygen atoms of water molecules in the liquid phase.

Two reasons can be considered for this difficulty. One reason is that the Hn2 site is surrounded by the JW and C32 hydrophobic sites. Thus, the water molecules do not approach the region including these three sites easily.

The other reason is the motion of the sites. As shown in Fig. 3a and b, the *x*-coordinates of the JW and Hn2 sites fluctuated with time. The period of the fluctuation was approximately 7 ps, which is

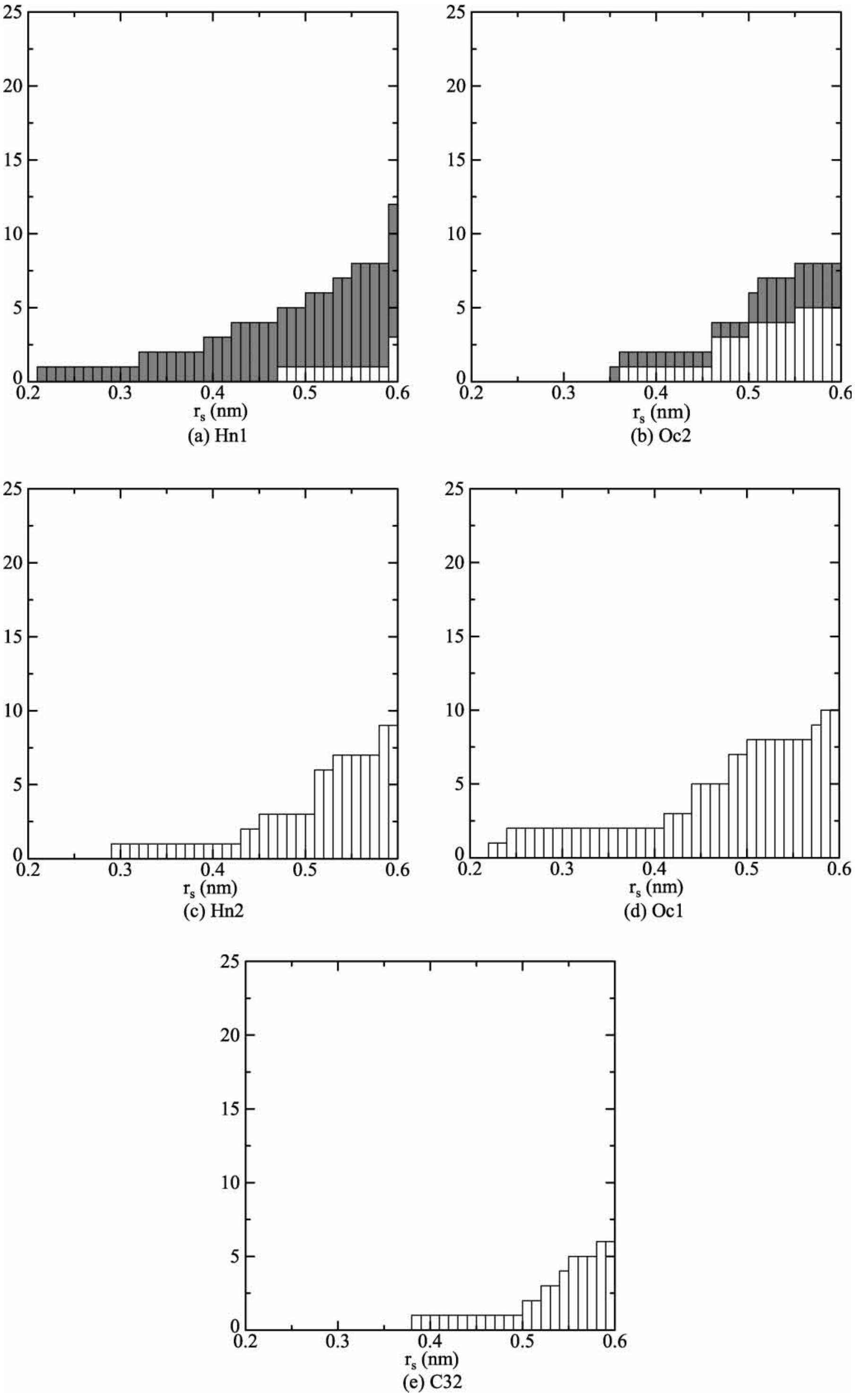

FIGURE 7 Number of atoms inside spherical shell in Case 2.

the same order of magnitude for the mean lifetime of the libration state for the hydrogen bond in the clusters of water molecules ($1-6$ ps) [16]. This fluctuation disturbed the cluster formation or the hydrogen bond between water molecules or that between a water molecule and the Oc1 and Hn2 sites. This situation is drawn schematically in Fig. 8.

A similar situation was obtained in Case 2. The C31, Oc1, Hn2 and C32 sites were farther from the ice nucleus than the other sites for the period of 30–120 ps as shown in Fig. 4. The Oc1 site was

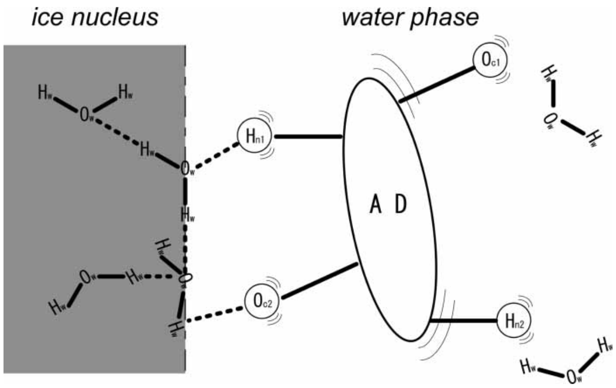

FIGURE 8 Interaction between Oc and Hn sites and water molecules.

surrounded by the C31 and C32 hydrophobic sites. No oxygen atom was inside the spherical region of $r_s = 0.26\,\text{nm}$ for the Hn2 site through this period except at 80 and 130 ps when one oxygen atom for a water molecule in the liquid phase was inside this region (figure omitted).

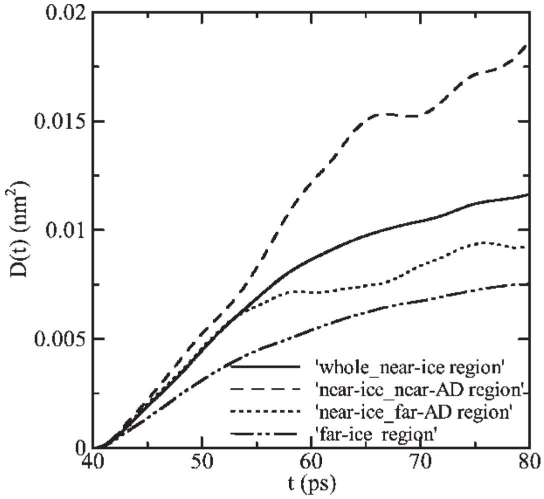

(a)40-80ps

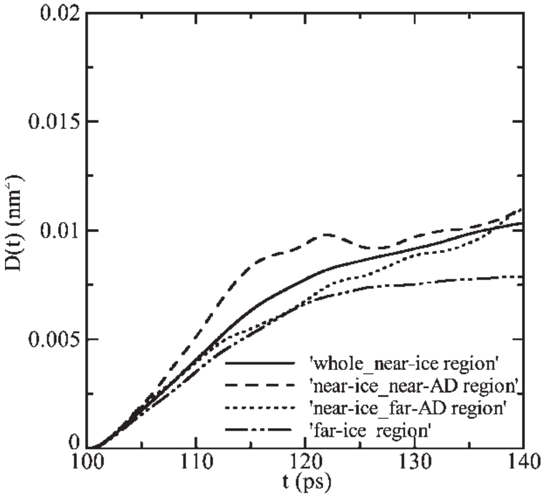

(b)100-140ps

FIGURE 9 Self-diffusion functions in Case 1.

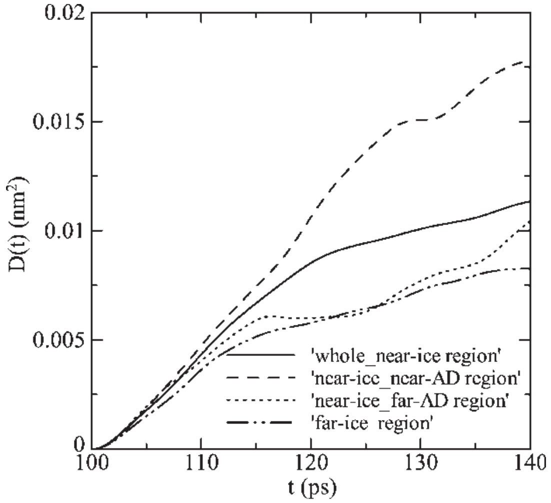

100-140ps

FIGURE 10 Self-diffusion functions in Case 2.

Diffusion of Water Molecules

The water molecules disturbed by the sites of the AD molecules can affect other water molecules. This was examined by the self-diffusion function of water molecules. Figure 9 exhibits the self-diffusion functions of water molecules in the near-ice region of the liquid phase in the periods of 40–80 and 100–140 ps in Case 1. The self-diffusion function of water molecules in the region (near an upper corner of the computational domain ($0 \le x \le 2.245$, $0 \le y \le 2.333$, $0 \le z \le 2.200\,\text{nm}$; hereafter called far-ice region), which is far from the nucleus and AD molecule in the domain, is drawn with the two-dot chain line. The function for all the water molecules in the near-ice region is drawn with the solid line. The function for the molecules in the near-ice–far-AD region is drawn with the dotted line. The final values of the function in the profiles are shown in Table VII. The function for the molecules in the near-ice–far-AD region takes slightly higher values than that for the molecules in the far-ice region, but takes lower values than that for all the molecules in the near-ice region. On the other hand, the function for the molecules in the near-ice-near-AD region drawn with the broken line takes the highest values. A similar result was obtained in Case 2 as shown in Fig. 10 and Table VI. Therefore, the AD molecule enhances the diffusion of the water molecules in the vicinity of the $\{1\,0\,\bar{1}\,0\}$ prism plane and the AD molecule.

Orientation of Water Molecules near the Prism Planes

We examined the angles of water molecules to the oxygen atoms on the prism planes in order

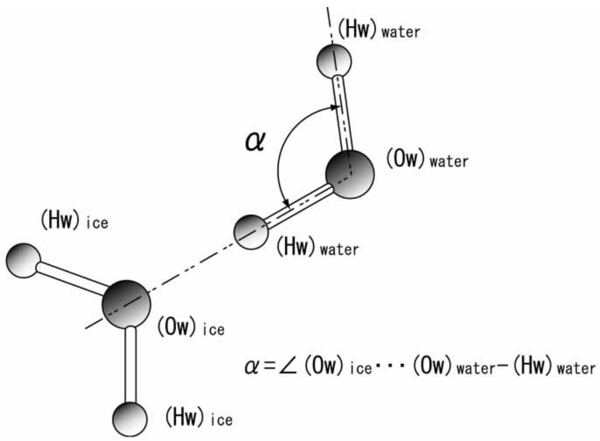

(a) definition of angle

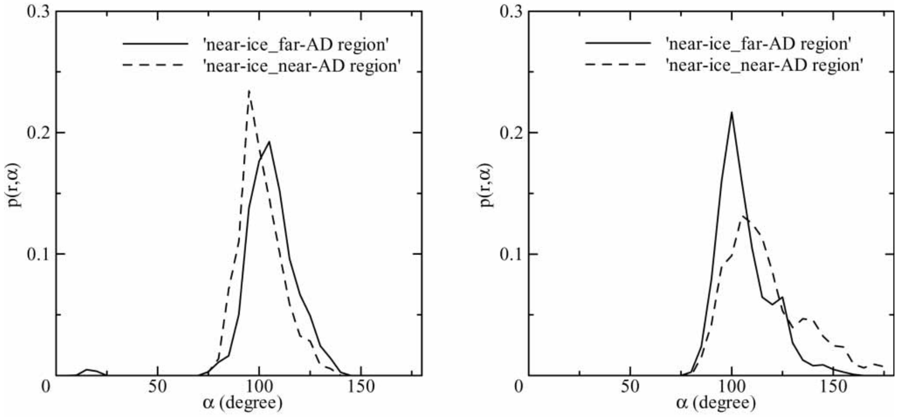

(b) Case 1 (c) Case 2

FIGURE 11 Angular distribution function.

to understand the indirect effect of the AD molecule on the adsorption of water molecules far from the AD molecule. Figure 11a shows the angle α among the oxygen atom on the prism plane $(\mathrm{Ow})_{\mathrm{ice}}$, the oxygen atom of water molecule Ow within a spherical shell whose radius from $(\mathrm{Ow})_{\mathrm{ice}}$ is in the range of $r_{p1} - r_{p2}$ and the hydrogen atom of the molecule Hw2 located farther from the prism plane than the other hydrogen atom Hw1. We set $r_{p1} = 0.265$ and $r_{p2} = 0.285\,\mathrm{nm}$ because the middle value is approximately equal to the distance between the oxygen atoms inside the ice nucleus (the distance of (Ow═Hw···Ow) is 0.276 nm, as is calculated from the values in Table VI). If α is 104 degrees, Hw1 is on the line between $(\mathrm{Ow})_{\mathrm{ice}}$ and Ow, and thus the hydrogen bond is highly expected between Hw1 and $(\mathrm{Ow})_{\mathrm{ice}}$. If α is far from 104 degrees, this hydrogen bond is not expected. Figures 11b and c indicate the probability distribution for α in Case 1 and Case 2, respectively. The probability is defined as follows:

$$p(r, \alpha) = \frac{n(r_{p1} \leq r \leq r_{p2}, \alpha)}{\sum_{\alpha=0^\circ}^{180^\circ} n(r_{p1} \leq r \leq r_{p2}, \alpha)}, \tag{4}$$

where n is the number of water molecules whose oxygen atoms are located inside the spherical shell mentioned above. These figures depict that the fraction of the angles, except for 100–105 degrees in the case of far-AD region, is lower than that in

TABLE VII Final values for the profiles of self-diffusion function

Figures	*t (ps)*	*Region*	*D(t) (nm^2)*
Fig. 9a	80	Whole–near-ice region	0.0116
		Near-ice–near-AD region	0.0187
		Near-ice–far-AD region	0.0092
		Far-ice region	0.0075
Fig. 9b	140	Whole–near-ice region	0.0103
		Near-ice–near-AD region	0.0110
		Near-ice–far-AD region	0.0109
		Far-ice region	0.0079
Fig. 10	140	Whole–near-ice region	0.0113
		Near-ice–near-AD region	0.0178
		Near-ice–far-AD region	0.0104
		Far-ice region	0.0083

the case of near-AD region. This shows that the possibility of hydrogen bond between the oxygen atom on the prism plane and the hydrogen of water molecule decreased due to the presence of the AD molecule.

CONCLUSIONS

The molecular dynamics simulation was carried out in order to understand the interaction among the AD molecule, the water molecules in the ice nucleus and those in the liquid phase. The main conclusions obtained are as follows.

(1) The Oc2 site and the Hn1 site of the AD molecule moved to the surface of the ice nucleus. The minimum distance between the Hn1 site and the oxygen atom of the ice lattice on the prism plane is shorter than that of the hydrogen bond. Thus, the hydrogen bond of Ow···Hn1 is expected.
(2) On the other hand, the minimum distance between the Oc2 site and the hydrogen atom of the lattice was longer than that of the hydrogen bond. This is partly because the sites do not match the lattice completely and partly because the hydrogen atom is more inside the nucleus than the oxygen atom of the lattice. Thus, the hydrogen bond of Hw···Oc2 is not expected.
(3) These interactions allow the gradual rotation and gradual slide on the prism surface of the AD molecule.
(4) This behavior of the AD molecule leads to time change in the positions of the Oc1 and Hn2 sites pointing away from the $\{10\bar{1}0\}$ prism plane. This causes the diffusion of water molecules.
(5) The motion of AD molecule prevents the hydrogen atoms of water molecules from bonding with the oxygen atoms in the ice lattice on the prism plane.

References

[1] Li, B. and Sun, D.W. (2001) "Novel methods for rapid freezing and thawing of foods—a review", *J. Food Eng.* **54**, 175.
[2] Yang, D.S.C., Sax, M., Chakrabatty, A. and Hew, C.L. (1988) "Crystal structure of an antifreeze polypeptide and its mechanistic implications", *Nature* **333**, 232.
[3] Yeh, Y. and Feeney, R.E. (1996) "Antifreeze proteins: structures and mechanisms of function", *Chem. Rev.* **96**, 601.
[4] Chao, H., Houston, M.E., Jr., Hodges, R.S., Kay, C.M., Sykes, B.D., Loewn, M.C., Davies, P.L. and Sönnichsen, F.D. (1997) "A diminished role for hydrogen bonds in antifreeze protein binding to ice", *Biochemistry* **36**, 14652.
[5] Haymet, A.D.J., Ward, L.G. and Harding, M.M. (1999) "Winter flounder 'antifreeze' proteins: synthesis and ice growth inhibition of analogues that probe the relative importance of hydrophobic and hydrogen-bonding interactions", *J. Am. Chem. Soc.* **121**, 941.
[6] Dalal, P., Knickelbein, J., Haymet, A.D.J., Sönnichsen, F.D. and Madura, J.D. (2001) "Hydrogen bond analysis of type 1 antifreeze protein in water and the ice/water interface", *Phys. Chem. Commun.* **4**, 32.
[7] DeLuca, C.I., Davies, P.L., Ye, Q. and Jia, Z. (1998) "The effects of steric mutations on the structure of type III antifreeze protein and its interaction with ice", *J. Mol. Biol.* **275**, 515.
[8] Yokoyama, T. and Hagiwara, Y. (2003) "Molecular dynamics simulation for the mixture of water and an ice nucleus", *Mol. Simul.* **29**, 235.
[9] Hayward, J.A. and Reimers, R. (1997) "Unit cells for the simulation of hexagonal ice", *J. Chem. Phys.* **106**, 1518.
[10] Jorgensen, W.J., Chandrasekhar, J., Madura, J.D., Impey, R.W. and Klein, M.L. (1983) "Comparison of simple potential functions for simulating liquid water", *J. Chem. Phys.* **79**, 926.
[11] Frenkel, D. and Smit, B. (1996) *Understanding Molecular Simulation* (Academic Press, San Diego).
[12] Gear, C.W. (1971) *Numerical Initial Value Problems in Ordinary Differential Equations* (Prentice-Hall, Englewood Cliffs).
[13] Jorgensen, W.J. and Tirado-Rives, J. (1988) "The OPLS potential functions for proteins: Energy minimizations for crystals of cyclic peptides and crambin", *J. Am. Chem. Soc.* **110**, 1657.
[14] Gould, I.R., Cornell, W.D. and Hillier, I.H. (1994) "A quantum mechanical investigation of the conformational energetics of the alanine and glycine dipeptides in the gas phase and in aqueous solution", *J. Am. Chem. Soc.* **116**, 9250.
[15] Kalko, S.G., Guàrdia, E. and Padró, J.A. (1999) "Molecular dynamics simulation of the hydration of the alanine dipeptide", *J. Phys. Chem.*, **103B**, 3935.
[16] Keutsch, F.N. and Saylally, R.J. (2001) "Water clusters: untangling the mysteries of the liquid, one molecule at a time", *Proc. Natl Acad. Sci. USA* **98**, 10533.